

# HAFNIUM-BASED BULK METALLIC GLASSES FOR KINETIC ENERGY PENETRATORS

Laszlo J. Kecskes,\* Brian T. Edwards, and Robert H. Woodman  
Weapons and Materials Technology Directorate  
AMSRD-ARL-WM-MB  
U.S. Army Research Laboratory  
Aberdeen Proving Ground, MD 21005-5069

## ABSTRACT

A new family of quinary, hafnium-based, bulk-metallic-glass-forming alloys has been developed for use in composite kinetic-energy penetrators. The alloys are based on an invariant point identified in the hafnium-copper-nickel ternary system. They are denser than zirconium-based glass-forming compositions, and exhibit a higher reduced glass-transition temperature than alloys prepared by 1:1 hafnium substitution into the zirconium-based alloys. The combination of density and glass-forming ability exhibited by this alloy moves the composite technology closer to being a viable substitute for depleted-uranium penetrators.

## 1. INTRODUCTION

### 1.1 Criterion for Effective Kinetic Energy Penetrator Performance

The lethality of depleted uranium-based (DU) and tungsten-nickel-iron (W-Ni-Fe) composite kinetic energy (KE) munitions is primarily ascribed to their high densities (U:  $\rho = 18.95 \text{ g/cm}^3$ , and W:  $\rho = 19.3 \text{ g/cm}^3$ , respectively). Additionally, DU's material characteristics give it greater penetration ability than W-Ni-Fe. The increased performance is attributed to a localized flow-softening behavior, more commonly referred to as adiabatic shear (AS) (Magness and Farrand, 1990). Localization occurs when the rate of thermal softening exceeds that of the rate of strain and strain-rate hardening. In ballistic tests with semi-infinite targets, the transformed zones tend to occur at oblique planes with respect to the penetrator-target interface that renders the DU alloy penetrator, unlike W-Ni-Fe, able to maintain a "chiseled-nose" shape favorable for enhanced penetration. However, environmental hazards and the cleanup of spent munitions impose additional costs on the use of DU.

A long-standing goal of current research is to achieve localized flow softening in non-DU materials. Conventional W-Ni-Fe composites are two-phase composites of nearly unalloyed W particles embedded in a Ni-alloy matrix. Because the W phase itself is very resistant to AS localization, efforts over the past decade have primarily focused on replacing the Ni-alloy matrix

with one having a greater susceptibility to AS failure.

As conceived, this W-based composite would combine the desirable properties of DU (*i.e.*, increased penetration and AS) and W (*i.e.*, density and non-toxicity) as a new class of high density, high strength, and high hardness KE penetrator. It is hoped that, by emulating the preferred erosion behavior in a comparable-density composite, the ballistic performance of DU penetrators can be matched.

### 1.2 Bulk Metallic Glass Alloys for Kinetic Energy Penetrator Applications

Alongside other possible candidate matrix materials, such as titanium (Ti), zirconium (Zr), hafnium (Hf), or certain steels with strong shear-localization susceptibility, the use of bulk metallic glasses (BMGs) has also been suggested. Unlike typical metals, BMGs do not have a crystalline structure. Their disordered atomic arrangement results in unusual mechanical behaviors. For example, when subjected to a compressive mechanical load, the BMG deforms by shear localization and fracture, in a similar manner to that exhibited by DU alloys at impact.

Shear localization in BMGs was first reported in Zr alloys which have densities of  $\sim 6.7 \text{ g/cm}^3$  (Bruck et al., 1994; Bruck, et al., 1996). Because of its low density, a Zr-alloy BMG alone would be ineffective as a penetrator material. However, it has been suggested that the combination of W with a BMG matrix would achieve the required combination of density and deformation mechanism to compete with DU. Nevertheless, the use of the low-density Zr alloy limits composites to densities  $\sim 15.5 \text{ g/cm}^3$ .

An alloy of sufficient density and glass-forming ability (GFA) is thus crucial to matching the performance of DU. GFA refers to the fact that the nature of metallic glasses restricts the sizes in which they can be made. Any metal can be prepared with a glass structure, provided that it can be cooled (quenched) from a melt rapidly enough. In practice, most metals and alloys require quench rates so high that glasses of metals and alloys are typically thin ribbons or foils. BMGs are prepared from alloys, which

Report Documentation Page			Form Approved OMB No. 0704-0188		
Public reporting burden for the collection of information is estimated to average 1 hour per response, including the time for reviewing instructions, searching existing data sources, gathering and maintaining the data needed, and completing and reviewing the collection of information. Send comments regarding this burden estimate or any other aspect of this collection of information, including suggestions for reducing this burden, to Washington Headquarters Services, Directorate for Information Operations and Reports, 1215 Jefferson Davis Highway, Suite 1204, Arlington VA 22202-4302. Respondents should be aware that notwithstanding any other provision of law, no person shall be subject to a penalty for failing to comply with a collection of information if it does not display a currently valid OMB control number.					
1. REPORT DATE <b>00 DEC 2004</b>		2. REPORT TYPE <b>N/A</b>		3. DATES COVERED <b>-</b>	
4. TITLE AND SUBTITLE <b>Hafnium-Based Bulk Metallic Glasses For Kinetic Energy Penetrators</b>				5a. CONTRACT NUMBER	
				5b. GRANT NUMBER	
				5c. PROGRAM ELEMENT NUMBER	
6. AUTHOR(S)				5d. PROJECT NUMBER	
				5e. TASK NUMBER	
				5f. WORK UNIT NUMBER	
7. PERFORMING ORGANIZATION NAME(S) AND ADDRESS(ES) <b>Weapons and Materials Technology Directorate AMSRD-ARL-WM-MB U.S. Army Research Laboratory Aberdeen Proving Ground, MD 21005-5069</b>				8. PERFORMING ORGANIZATION REPORT NUMBER	
9. SPONSORING/MONITORING AGENCY NAME(S) AND ADDRESS(ES)				10. SPONSOR/MONITOR'S ACRONYM(S)	
				11. SPONSOR/MONITOR'S REPORT NUMBER(S)	
12. DISTRIBUTION/AVAILABILITY STATEMENT <b>Approved for public release, distribution unlimited</b>					
13. SUPPLEMENTARY NOTES <b>See also ADM001736, Proceedings for the Army Science Conference (24th) Held on 29 November - 2 December 2005 in Orlando, Florida. , The original document contains color images.</b>					
14. ABSTRACT					
15. SUBJECT TERMS					
16. SECURITY CLASSIFICATION OF:			17. LIMITATION OF ABSTRACT <b>UU</b>	18. NUMBER OF PAGES <b>18</b>	19a. NAME OF RESPONSIBLE PERSON
a. REPORT <b>unclassified</b>	b. ABSTRACT <b>unclassified</b>	c. THIS PAGE <b>unclassified</b>			

yield glass at much lower cooling rates, and can thus be made in larger dimensions. Increasing alloy density without compromising GFA thus poses a challenge to the metallurgist.

In addition to being high, the quench rates used in metallic glass preparation are difficult to measure directly. However, an easily measured parameter of the glass, the reduced glass-transition temperature ( $T_{rg}$ ), correlates with quench rate. Typically, the larger  $T_{rg}$  is, the smaller the critical cooling (or quench) rate needs to be.  $T_{rg}$  is the glass-transition temperature,  $T_g$ , normalized to the liquidus temperature,  $T_l$ , of the alloy. Both parameters can be measured with commonly available thermal analysis equipment. A  $T_{rg}$  between 0.63 and 0.67 represents a BMG alloy with good GFA (Johnson, 1999).

### 1.3 Composition Rules for Bulk Metallic Glass Alloys

A large  $T_{rg}$  translates into a low  $T_l$  value for a given alloy family. Typically in multicomponent systems, the compound with the lowest  $T_l$  corresponds to a eutectic composition.

At the eutectic composition, there is a strong competition between several crystalline phases to nucleate, grow, and accommodate one another in the solid phase. The required atomic rearrangement for crystallization and solidification takes time. Therefore, the atoms may be in a thermodynamically more favorable state if they remain in the liquid. If being in the liquid phase is more stable, the stability would be manifested as a greater depression in the melting point (Johnson, 1999). Increased stability in the liquid near a eutectic composition could then also be interpreted as a higher propensity for bypassing crystallization, and hence improved GFA as well.

There is considerable discord in the BMG community regarding the location of the ideal alloy composition that has an optimum GFA. Arguments for the use of the eutectic composition (Li, 2001) have been opposed with examples of hypo- or hypereutectic compositions (Wang et al., 2004; Xu et al., 2004).

In addition to locating systems with deep eutectics, other topological and empirical rules also aid BMG formation. These include the use of at least three elements, dissimilar crystal structures, negative heats of mixing, and large- and small-sized atoms. Such factors are designed to increase the competition between phases and raise the chemical disorder in the liquid, thereby destabilizing the formation processes of possible crystalline phases. Any complication, frustration, or confusion of the solidification process near the eutectic composition, cause the nucleation kinetics to become more sluggish and crystallization then can be avoided.

### 1.4 Zr- and Hf-Based Bulk Metallic Glass Alloys

Our initial efforts to develop higher-density BMGs centered on two quinary alloys of Zr with good GFA:  $Zr_{52.5}Ti_5Cu_{17.9}Ni_{14.6}Al_{10}$  (Vit105) and  $Zr_{57}Ti_5Cu_{20}Ni_8Al_{10}$  (JHU Zr57). It was felt that, based on the strong chemical similarities between Zr and Hf, direct substitution of Hf for Zr would be a straightforward approach. Replacing Zr with Hf in 20-at. % increments, we produced alloy ingots with densities ranging from 6.7 to 11.1 g/cm<sup>3</sup>.

We were able to prepare glass for all compositions in the  $(Hf_xZr_{1-x})_{52.5}Ti_5Cu_{17.9}Ni_{14.6}Al_{10}$  series. In contrast, in the  $(Hf_xZr_{1-x})_{57}Ti_5Cu_{20}Ni_8Al_{10}$  series, compositions of  $x > 0.6$  could not be quenched to a uniform glass structure (Kecskes et al., 2002). As shown in Fig. 1, in the  $(Hf_xZr_{1-x})_{52.5}Ti_5Cu_{17.9}Ni_{14.6}Al_{10}$  series,  $T_{rg}$  declined from 0.628 ( $x = 0$ ) to 0.608 ( $x = 1$ ) with increasing  $x$ . The decline from an initial  $T_{rg}$  of 0.588 ( $x = 0$ ) was more pronounced in the other series.

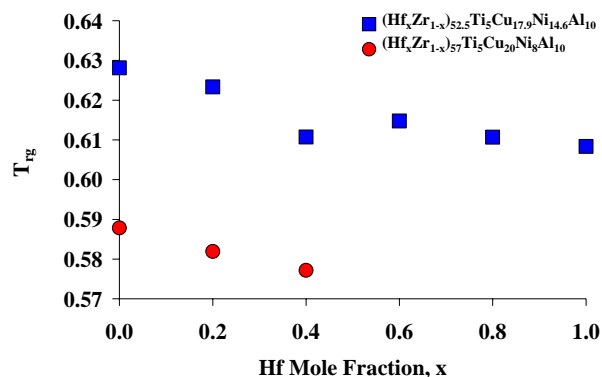


Fig. 1.  $T_{rg}$  of  $(Hf_xZr_{1-x})_{52.5}Ti_5Cu_{17.9}Ni_{14.6}Al_{10}$  and  $(Hf_xZr_{1-x})_{57}Ti_5Cu_{20}Ni_8Al_{10}$  BMGs. Note the gradual decline with increasing Hf mole fraction.

Obviously, this approach would not result in an improvement in GFA. Subsequently, we observed that the Zr:Cu:Ni ratio of  $Zr_{52.5}Ti_5Cu_{17.9}Ni_{14.6}Al_{10}$  (Vit105),  $Zr_{57}Nb_5Cu_{15.4}Ni_{12.6}Al_{10}$  (Vit106), or  $Zr_{57}Ti_5Cu_{20}Ni_8Al_{10}$  (JHU Zr57) alloy is near the Zr-Cu-Ni ternary eutectic point (Fig. 2). It was hypothesized that the low  $T_{rg}$  of the substitutionally obtained Hf alloys was attributed to being too far from the corresponding Hf-Cu-Ni ternary eutectic point. However, a Hf alloy with Hf:Cu:Ni ratio near the Hf-Cu-Ni eutectic point would be a good glass-former.

Because no ternary Hf-Cu-Ni phase diagram could be found in the literature, we undertook a study of the Hf-Cu-Ni phase equilibria. Once the invariant points were identified, we applied the BMG formation rules to develop a Hf alloy with improved GFA. We used, differential thermal analysis, a well-established technique, for the determination of phase equilibria in alloys (Pope

and Judd, 1977). We also relied on X-ray diffraction, scanning and transmission electron microscopies to determine and verify the structure of the alloyed and glassy materials. We report these results here.

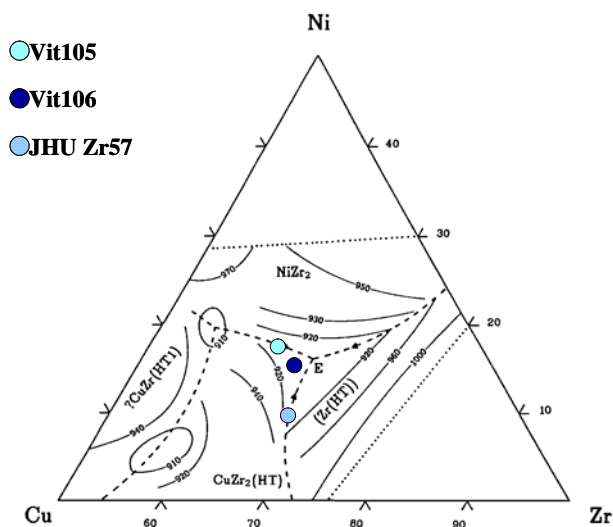


Fig. 2. Zr:Cu:Ni ratios of common Zr alloys, mapped onto the two-dimensional plane projection of the Zr-Cu-Ni liquidus surface (taken from Takeuchi, 1968). Note all are near the eutectic point (E).

## 2. EXPERIMENTAL PROCEDURES

### 2.1 Invariant-Point Identification

Identifying invariant points in the Hf-Cu-Ni system entailed synthesizing ternary compositions, and measuring their melting behavior using differential thermal analysis. Elemental metals were pickled in an acidic solution, and arc melted under a Ti-gettered, partial-vacuum argon atmosphere. The ingot buttons were flipped and remelted several times (typically 6 melts) to ensure complete alloying of the elements.

Thermal analysis was conducted using a Netzsch Instruments STA 409C differential thermal analyzer (DTA) configured with a high-temperature (1600 °C) furnace, Type S thermocouples, graphite crucibles, and an argon atmosphere. Heating rates were 10 °C/min. To establish good thermal contact between the crucible and the sample, alloy samples were melted, allowed to cool, and solidify in the DTA furnace prior to the analysis scan.

Backscatter scanning electron microscopy (SEM) was used to examine the phase assemblage of samples cooled in the DTA. We used a Hitachi S-4700 field-emission scanning electron microscope, with a tungsten electron source and a YAG backscatter detector.

### 2.2 Quaternary and Quinary Alloy Development

Once the invariant point was identified, further alloying additions were made. The goal of alloying additions was to lower the liquidus temperature while retaining the congruent nature of the melt.

5 and 10 atomic % (at. %) Ti, niobium (Nb), aluminum (Al), and chromium (Cr) were substituted for Hf at the invariant composition ( $\text{Hf}_{55}\text{Cu}_{30}\text{Ni}_{15}$ , see Results and Discussion), or mixed proportionally while maintaining the Hf:Cu:Ni ratio fixed. In addition, a 15-at. %-Al, proportionally substituted ingot was prepared. The resulting ingots were subjected to the same thermal analysis procedure described above.

Glass-forming ability was determined by suction casting 3-mm-diameter rods. Suction casting was performed by arc-remelting ingot pieces in Ti-gettered purified argon, followed by drawing and quenching the melt into a water-cooled Cu mold. The suction-casting apparatus has been described elsewhere (Gu, et al., 2002).

### 2.3 Bulk Metallic Glass Characterization

Due to the high strengths and large elastic limits of metallic glasses, a simple screening procedure to determine whether or not a suction-cast rod might be glassy is to bend it in one's hands. If it breaks, it is not glass. All suction-cast rods were subjected to this test.

Segments of rods, which passed the initial screening, were subjected to differential scanning calorimetry analysis. To determine glass-transition temperature, the STA 409C was configured with an argon atmosphere, Type E thermocouples, and copper crucibles. Heating rate was 10 °C/min.

Alloy density was determined using the Archimedes method in water.

X-ray diffraction patterns were recorded using Philips PW 1729 x-ray generator, with a typical copper  $K_{\alpha}$  tube source, scintillation detector, and low-background sample holder. Scans were taken over a 2- $\theta$  scattering angle range of 20 to 120 °, with a step size of 0.025 °, and 5-s dwell time.

A sample of the suction-cast glass-forming alloy was thinned with an FEI-200 focused ion beam milling device until electron transparent, and examined using a 300-kV FEI Technai F30 high-resolution transmission electron microscope.

### 3. RESULTS AND DISCUSSION

#### 3.1 Invariant-Point Identification

Each point on the ternary Hf-Cu-Ni plot (Fig. 3) represents a composition for which an ingot was made and subjected to thermal analysis. The dashed lines represent a series of pseudo-binary compositions, wherein the mole fraction of the third component is fixed. The intersections of the dashed lines are compositions, which were observed to melt congruently. Figure 4 illustrates melting point data along these composition lines, indicating how the solidus and liquidus converge at one of these invariant points.

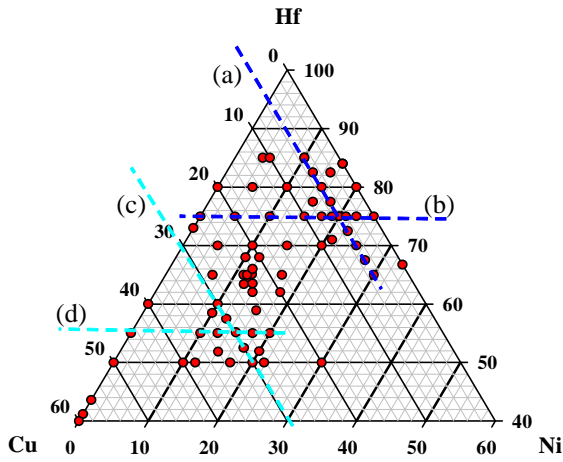


Fig. 3. The locus of all experimentally fabricated Hf-Cu-Ni alloy points, depicted on the Hf-Cu-Ni ternary composition triangle. The two sets of intersecting lines, labeled as (a) and (b), and (c) and (d), respectively, define the invariant points found in our study.

The DTA thermographs for  $\text{Hf}_{55}\text{Cu}_{30}\text{Ni}_{15}$  and  $\text{Hf}_{70}\text{Cu}_5\text{Ni}_{25}$  are exhibited in Fig. 5. It may be noted that although data in Fig. 4 infers that the invariant point is at  $\text{Hf}_{75}\text{Cu}_5\text{Ni}_{25}$ , the convergence of the solidus and liquidus occurs over a wider composition range. For clarity, heretofore, we designate the nominal eutectic composition as  $\text{Hf}_{70}\text{Cu}_5\text{Ni}_{25}$ . For  $\text{Hf}_{55}\text{Cu}_{30}\text{Ni}_{15}$ , the onset of melting was  $1150^\circ\text{C}$ , while the endpoint was at  $1165^\circ\text{C}$ . For  $\text{Hf}_{70}\text{Cu}_5\text{Ni}_{25}$ , they were  $1130$  and  $1144^\circ\text{C}$ , respectively. We have not yet developed a glass-forming alloy based on  $\text{Hf}_{70}\text{Cu}_5\text{Ni}_{25}$ , so we will limit our discussion to alloys based on  $\text{Hf}_{55}\text{Cu}_{30}\text{Ni}_{15}$ .

#### 3.2 Quaternary and Quinary Alloy Development

Figure 6 presents the thermographs for the 5 at. % Ti and 10 at. % Al alloying additions to  $\text{Hf}_{55}\text{Cu}_{30}\text{Ni}_{15}$ . The ingot compositions are  $\text{Hf}_{50}\text{Ti}_5\text{Cu}_{30}\text{Ni}_{15}$  and  $\text{Hf}_{49.5}\text{Cu}_{27}\text{Ni}_{13.5}\text{Al}_{10}$ . The concentrations of these elements

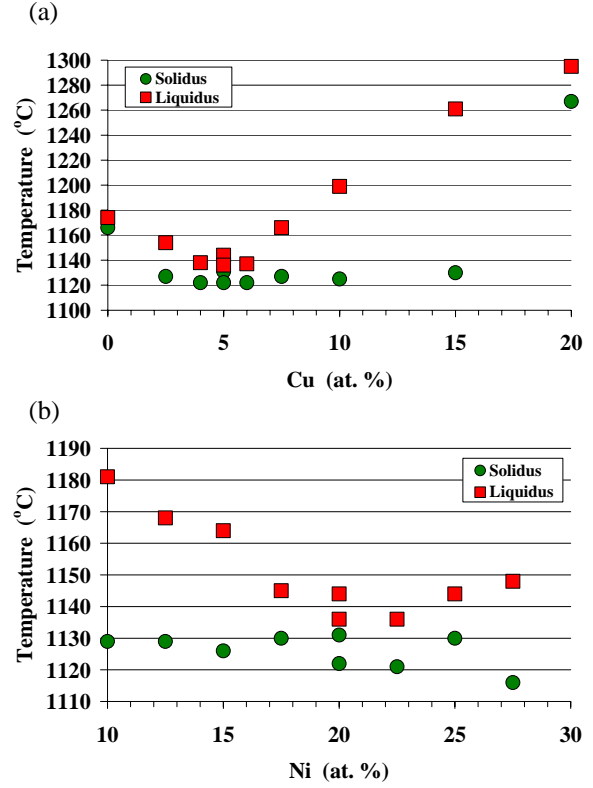


Fig. 4. Plots of solidus and liquidus vs. composition for (a)  $\text{Hf}_{75}\text{Cu}_x\text{Ni}_{25-x}$ , and (b)  $\text{Hf}_{95-x}\text{Cu}_5\text{Ni}_x$ .

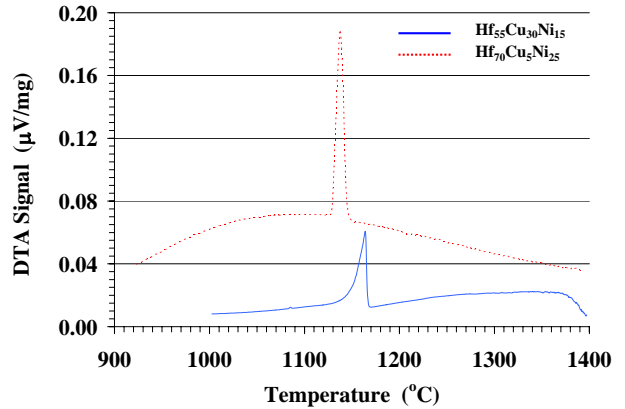


Fig. 5. DTA thermographs of the two congruently melting ternary alloys.

reduced the liquidus temperature of  $\text{Hf}_{55}\text{Cu}_{30}\text{Ni}_{15}$  as shown, while maintaining the congruent melting behavior. The other alloying elements (Nb and Cr) and other concentrations of Ti or Al elements resulted in moving the composition away from a congruent melt. The typical result of the other alloying additions was the appearance of a shoulder on the high-temperature side of the melting peak (not shown). This would be consistent with the persistence of a small amount of higher-melting-point

material after the initial melting began.

Because 5 at. % Ti and 10 at. % Al had the effect that they did in quaternary ingots, we prepared suction-cast rods of  $\text{Hf}_{44.5}\text{Ti}_5\text{Cu}_{27}\text{Ni}_{13.5}\text{Al}_{10}$ . Rods of this nominal composition passed the simple mechanical screening described above, and were subjected to the glass-characterization tests.

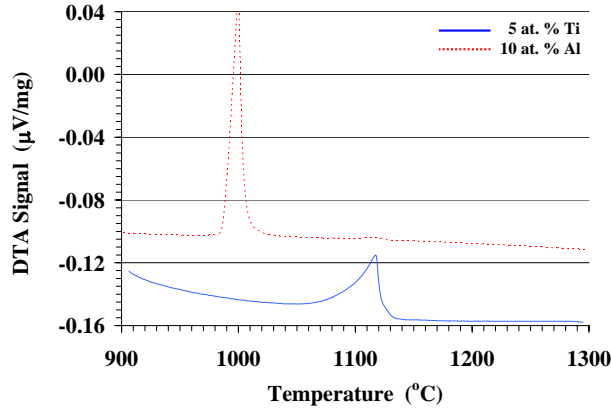


Fig. 6. Alloying effect of Ti and Al on the solidus and liquidus of  $\text{Hf}_{55}\text{Cu}_{30}\text{Ni}_{15}$ .

### 3.3 Metallic Glass Characterization

The density of the metallic glass is  $10.9 \text{ g/cm}^3$ . As shown in Fig. 7, the X-ray diffraction pattern from a suction casting exhibits a broad, diffuse ring with no Bragg peaks. A selected-area electron diffraction pattern, Fig. 8 (a), showed similar features. The corresponding bright-field, high-resolution image in Fig. 8 (b) reveals no evidence of crystallites or ordering. DTA determined  $T_g$  to be 500  $^{\circ}\text{C}$ ,  $T_i = 984^{\circ}\text{C}$ , making  $T_{rg} = 0.615$  (Fig. 9).

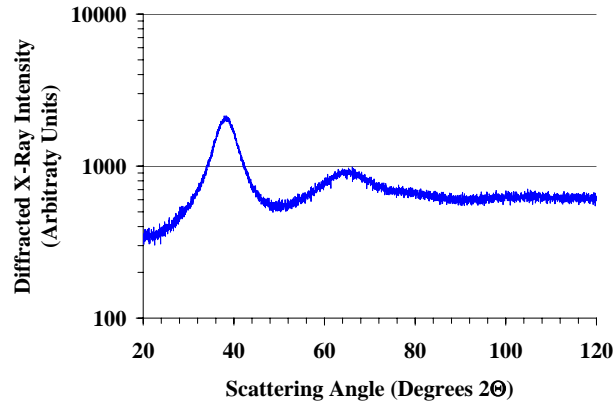
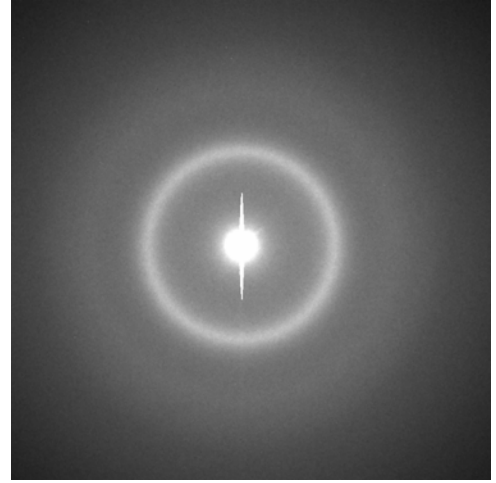


Fig. 7. X-ray diffractogram of the  $\text{Hf}_{44.5}\text{Ti}_5\text{Cu}_{27}\text{Ni}_{13.5}\text{Al}_{10}$  glass.

(a)



(b)

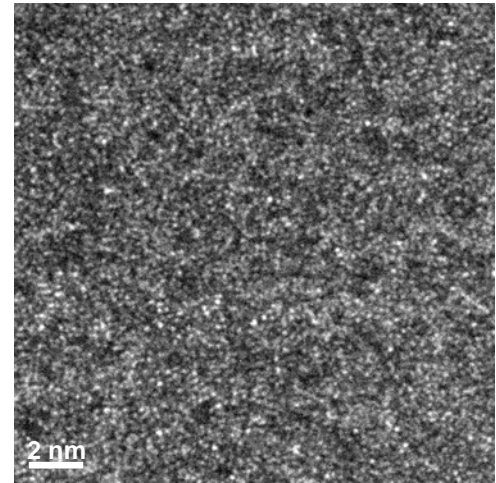


Fig. 8. Electron diffraction pattern and high-resolution transmission electron micrograph, shown in (a) and (b), demonstrate no long-range crystalline order in the alloy.

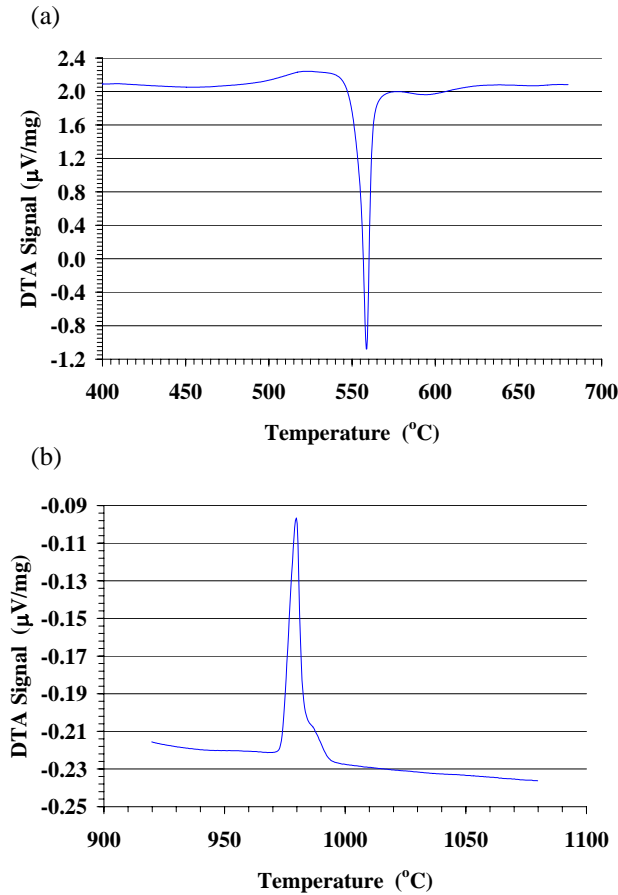


Fig. 9. DTA thermograms exhibiting a glass transition point and a single exothermic peak, shown in (a), and an endothermic peak defining the solidus and liquidus of the alloy in (b).

### 3.4 Detailed Study of $\text{Hf}_{55}\text{Cu}_{30}\text{Ni}_{15}$ Invariant Point

Attempts to reproduce the thermograph of Fig. 5 revealed a small endotherm at 1085  $^{\circ}\text{C}$  (not shown). Subsequent measurements revealed that this endotherm appears in most nearby compositions, including the compositions through which the dotted lines are drawn in Fig. 3. Figure 10 illustrates the variation of solidus and liquidus lines with composition for these alloys.

If the  $\text{Hf}_{55}\text{Cu}_{30}\text{Ni}_{15}$  were a eutectic, the liquidus would converge to the solidus at that composition (see Fig. 4). As is clear from Fig. 10, it does not. The presence of the small endotherm at 1085  $^{\circ}\text{C}$  also means that  $\text{Hf}_{55}\text{Cu}_{30}\text{Ni}_{15}$  is not a eutectic.

Backscattered SEM micrographs of a furnace-cooled ingot of  $\text{Hf}_{55}\text{Cu}_{30}\text{Ni}_{15}$  are exhibited in Fig. 11. It is clear from Fig. 11 (a) that the composition is off eutectic, although there is a eutectic microstructure present. The eutectic region probably corresponds to the 1085  $^{\circ}\text{C}$  endotherm observed in thermal analysis. Figure 11 (b) is

a higher magnification study of the eutectic region.

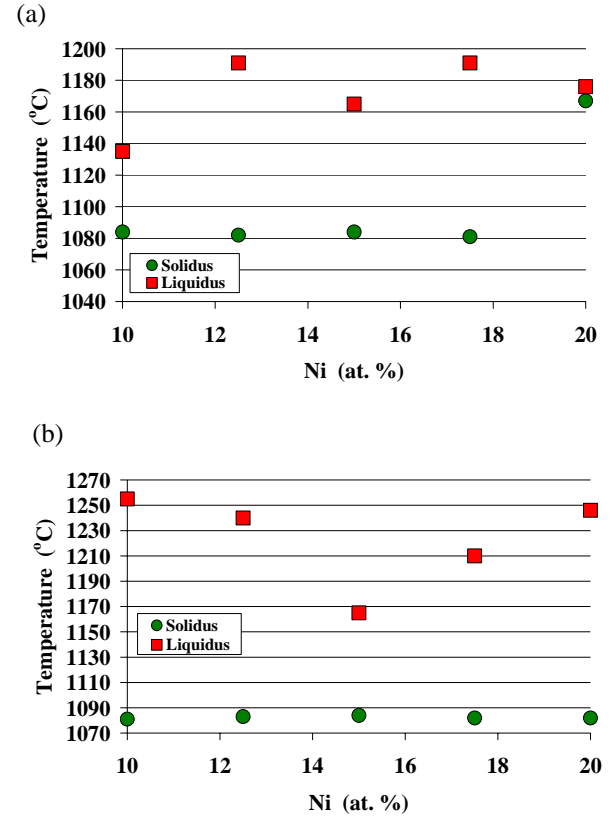
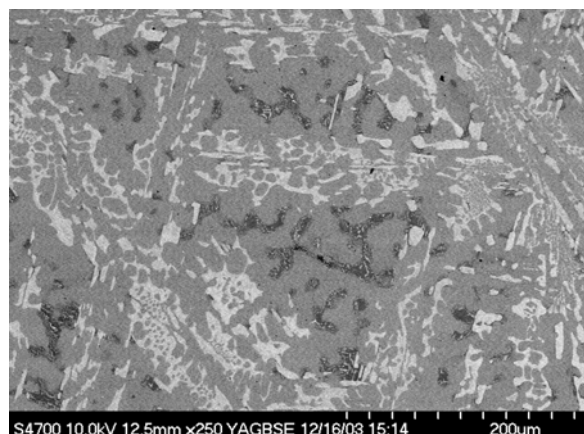


Fig. 10. Plots of solidus and liquidus *versus* composition for (a)  $\text{Hf}_{55}\text{Cu}_{45-x}\text{Ni}_x$ , and (b)  $\text{Hf}_{70-x}\text{Cu}_{30}\text{Ni}_x$ .

The fact that  $\text{Hf}_{55}\text{Cu}_{30}\text{Ni}_{15}$  is not a eutectic composition has important consequences for the development of metallic glasses. It appears from the asymmetric nature of the 1160  $^{\circ}\text{C}$  endothermic peak (Fig. 5) and the appearance of the microstructure that the peak most likely is a peritectic point resulting from the interaction of the a small amount of eutectic liquid with an incongruently melting compound. While such an alloy does not have the advantages that a eutectic would have for forming glass, peritectic points still involve considerable atomic rearrangement. If quenching is sufficiently rapid to prevent such rearrangement, it appears from the evidence presented here that peritectic points are also promising candidates for the development of glass-forming alloys. If this can be shown to be widely true, the opportunities for making bulk metallic glasses will have expanded greatly.

(a)



(b)

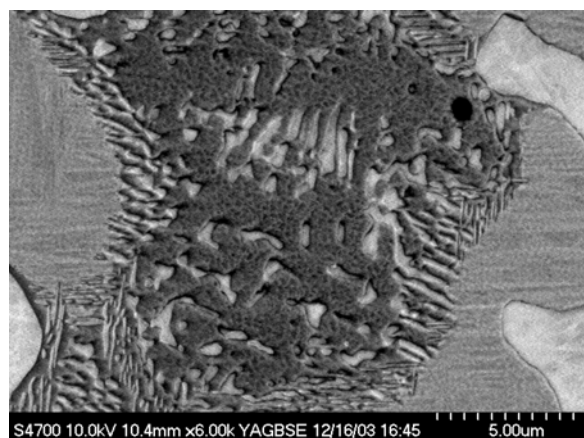


Fig. 11. Backscattered SEM micrographs of the  $\text{Hf}_{55}\text{Cu}_{30}\text{Ni}_{15}$  alloy sample with an overview shown in (a) and an enlarged view shown in (b).

## 6. CONCLUSIONS

The significance of this discovery in the development of high-density BMGs is twofold. First, it implies that a Hf-alloy BMG could be formed into bulk objects with dimensions equivalent to those only previously available to Zr-alloy BMGs. Second, and more importantly, it has enabled fabrication of  $17\text{-g/cm}^3$  composites, which approach the density of WHA KE penetrators. Ballistic tests of the first composites prepared showed penetration was more pronounced than would be expected from density alone.

## ACKNOWLEDGEMENTS

We would like to thank Prof. Y.H. Sohn (University of Central Florida, Orlando, FL) for preparing the high-resolution transmission electron microscopy specimen,

diffraction patterns, and micrographs. We would also like to acknowledge Ms. Minna Kim and Mr. George Dewing, both of ARL, for assistance in the preparation of alloys and metallographic samples. Finally, we are indebted to Mr. Bradley Klotz, also of ARL, for his assistance in the operation of the field-emission scanning electron microscope.

## REFERENCES

- Bruck, H.A., Christman, T., Rosakis, A.J., and Johnson, W.L., 1994: Quasi-Static Constitutive Behavior of  $\text{Zr}_{41.25}\text{Ti}_{13.75}\text{Ni}_{10}\text{Cu}_{12.5}\text{Be}_{22.5}$  Bulk Amorphous Alloy, *Scripta Metall. et Mater.*, **30**, 429-434.
- Bruck, H.A., Rosakis, A.J., and Johnson, W.L., 1996: The Dynamic Compressive Behavior of Beryllium Bearing Bulk Metallic Glasses, *J. Mater. Res.*, **11**, 503-511.
- Gu, X., Xing, L., and Hufnagel, T.C., 2002: Preparation and Glass Forming Ability of Bulk Metallic Glass  $(\text{Hf}_x\text{Zr}_{1-x})_{52.5}\text{Cu}_{17.9}\text{Ni}_{14.6}\text{Al}_{10}\text{Ti}_5$ , *J. Non-Cryst. Solids*, **311**, 77-82.
- Johnson, W.L., 1999: Bulk Glass-Forming Metallic Alloys: Science and Technology, *MRS Bulletin*, **24**, 42-56.
- Li, Y., 2001: A Relationship Between Glass-Forming Ability and Reduced Glass Transition Temperature Near Eutectic Composition. *Mater. Trans.*, **42**, 556-561.
- Keckes, L.J., Trevino, S.F., and Woodman, R.H., 2002: Glass-Forming Ability and Crystallization Behavior in High-Density Bulk Metallic Glasses, *Proc. of 2002 MRS Symp.*, 754, MRS, Warrendale, PA, 377-384.
- Magness, L.S. and Farrand, T.G., 1990: Deformation Behavior and Its Relationship to the Penetration Performance of High-Density KE Penetrator Materials, *Proc. 17th Army Science Conf.*, Durham, NC, 1990, Army Science Board, Washington, DC, **2**, 149-164.
- Pope, M.I. and Judd, M.D., 1977: *Differential Thermal Analysis*, Heyden and Son Ltd., Bellmawr, NJ, Ch. 6.
- Takeuchi, Y., Watanabe, M., Yamabe, S., and Wada, T., 1968: Eutektische Titan- und Zirkonium-Lote, *Metall.*, **22**, 8-15.
- Wang, D, Li, Y., Sun, B.B., Sui, M.L., Lu, K., and Ma, E., 2004: Bulk Metallic Glass Formation in the Binary Cu-Zr System, *Appl. Phys. Lett.*, **84**, 4029-4031.
- Xu, D., Lohwongwatana, B., Duan, G., Johnson, W.L., and Garland, C., 2004: Bulk Metallic Glass Formation in Binary Cu-Rich Alloy Series –  $\text{Cu}_{100-x}\text{Zr}_x$  ( $x = 34, 36, 38.2, 40$  at.%) and Mechanical Properties of Bulk  $\text{Cu}_{64}\text{Zr}_{36}$  Glass, *Acta Mater.*, **52**, 2621-2624.



# Hafnium-Based Bulk Metallic Glasses for Kinetic Energy Penetrators



**Laszlo J. Kecskes**, Brian T. Edwards, and Robert H. Woodman

Weapons and Materials Technology Directorate  
AMSRD-ARL-WM-MB  
U.S. Army Research Laboratory  
Aberdeen Proving Ground, MD 21005-5069

24<sup>th</sup> Army Science Conference  
Orlando, FL  
November 29-December 2, 2004

Laszlo Kecskes  
Army Science Conference #24 GO-03  
December 2, 2004



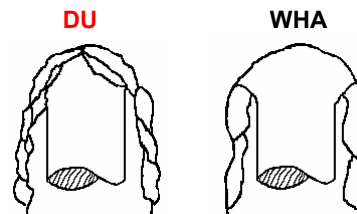
## Hf-Based BMGs Motivation



Develop enhanced tungsten-based kinetic energy penetrator materials that replicate the deformation and flow behavior of depleted uranium (DU) materials.


It is inherent that if imitation of the ballistic deformation behavior is successful, the ballistic performance will follow...

DU outperforms tungsten as localized deformation causes the bulging tip to remain sharp.




**Goal: Reproduce uranium-like behavior with non-uranium material**

Laszlo Kecskes  
Army Science Conference #24 GO-03  
December 2, 2004



## Hf-Based BMGs

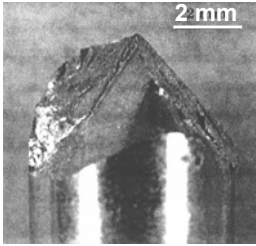
### Motivation



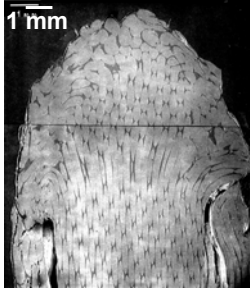
**Uranium-Like Behavior:** i.e., Self-Sharpening

ARO funded SBIR program at CalTech  
Zr-Ti-Cu-Ni-Be: castable bulk metallic glass alloy


'chisel' nose on monolithic BMG



reduced mushrooming on W-wire-reinforced-BMG composite




Laszlo Kecskes  
Army Science Conference #24 GO-03  
December 2, 2004

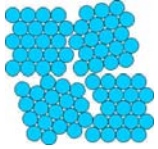


## Hf-Based BMGs

### Tutorial: History



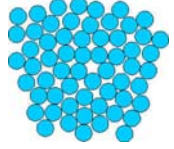
**Crystalline**



atoms arranged into a structure with order

versus

**Glassy**



atoms in liquid-like disordered arrangement

**Amorphous Structures:**


- **Types:**
  - 1960's: first metallic glass Au-Si by Klement et al. - **binary**
  - 1980's: Pd<sub>40</sub>Ni<sub>40</sub>P<sub>20</sub> - **ternary**
  - 1990's: Vitreloy1 (Zr<sub>41.2</sub>Ti<sub>12.8</sub>Ni<sub>10</sub>Cu<sub>12.5</sub>Be<sub>22.5</sub>) - **quinary**
- **Forms:**
  - Thin Films (nm) → Ribbon (μm) and Wire (μm)

Bulk Metallic Glasses (BMG) (mm)

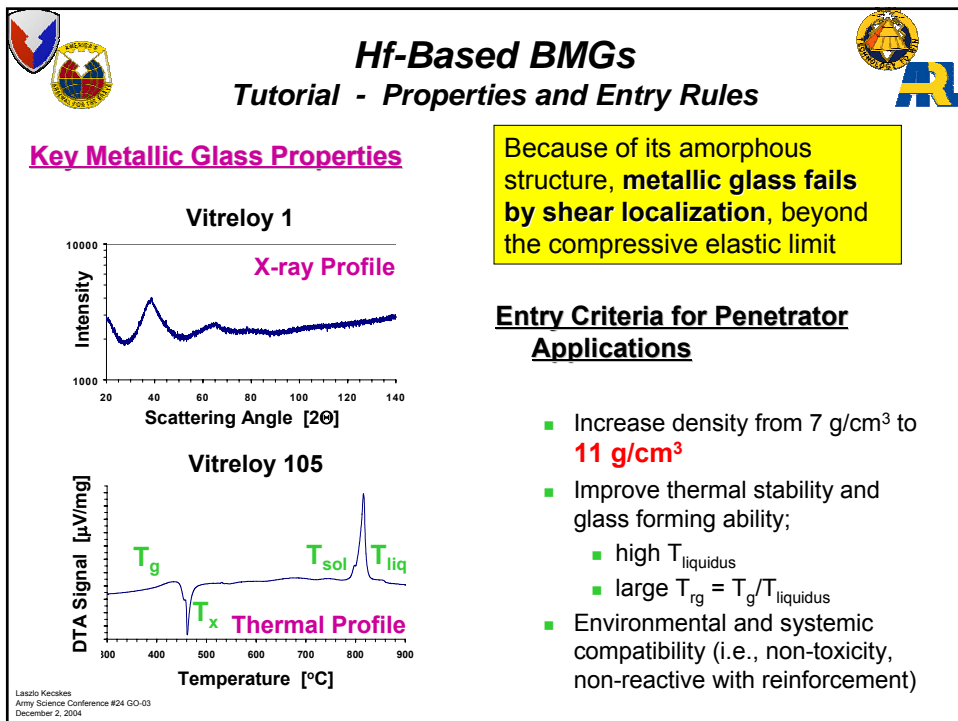
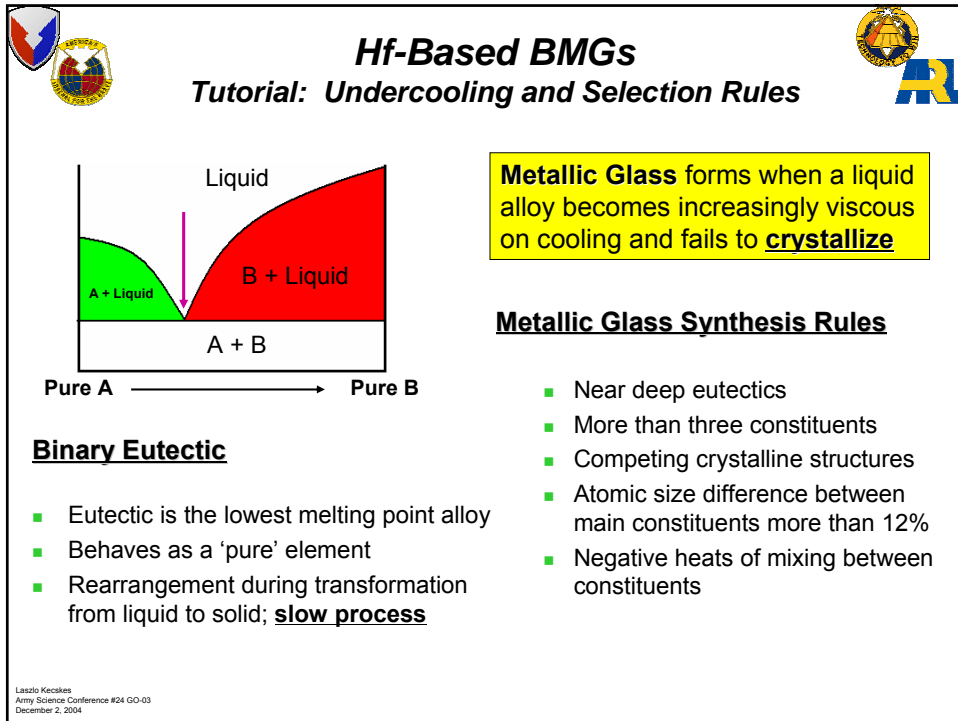
Cooling Rate

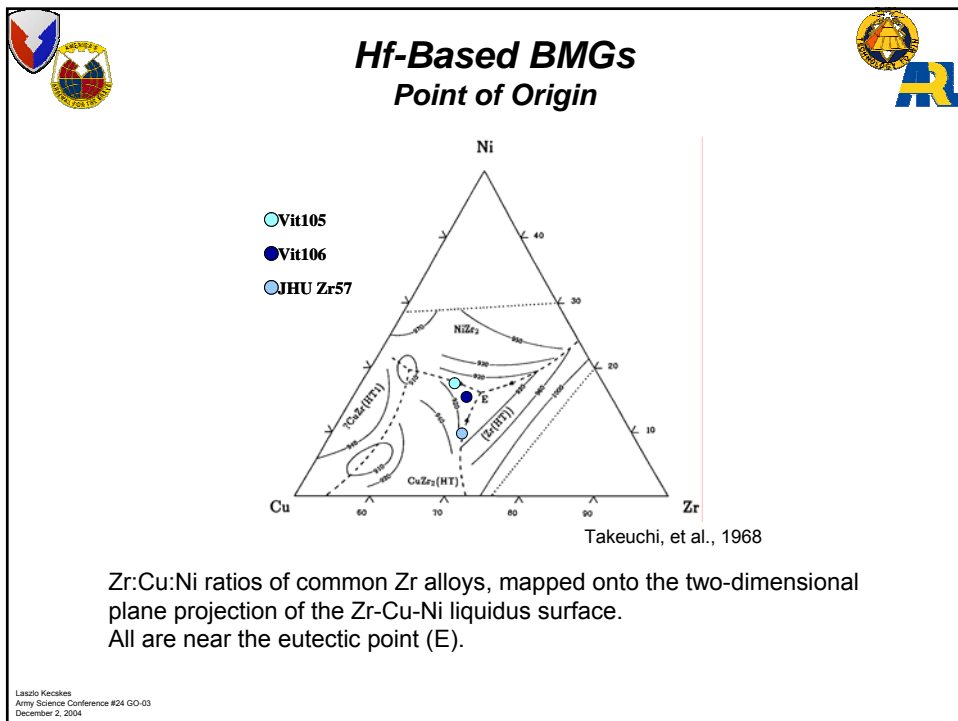
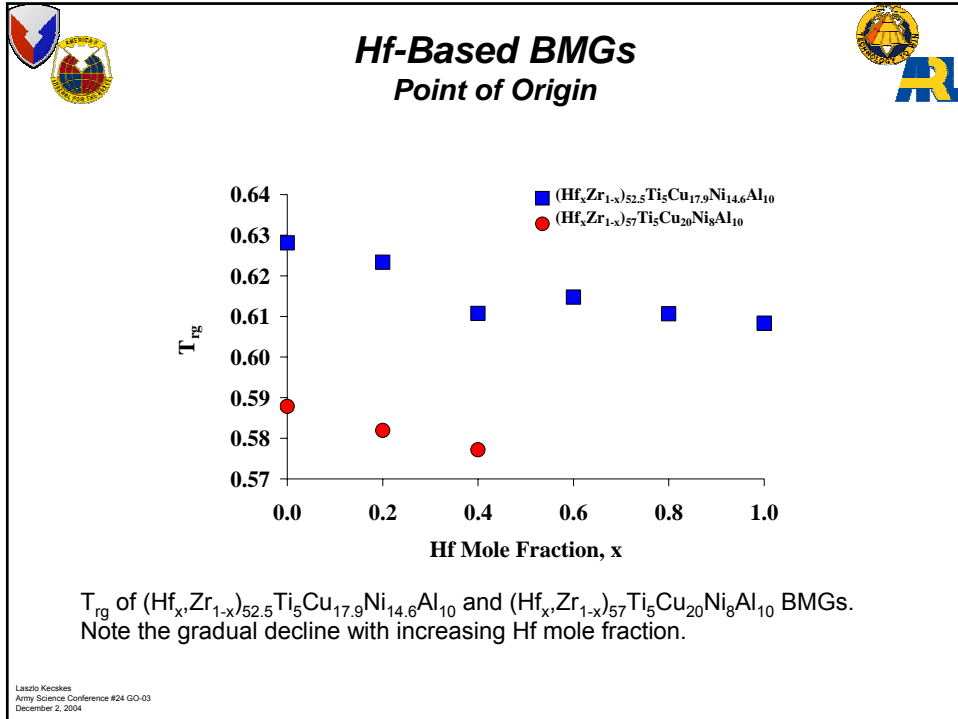
10<sup>6</sup> – 10<sup>5</sup> K/s

10 – 1 K/s



Laszlo Kecskes  
Army Science Conference #24 GO-03  
December 2, 2004

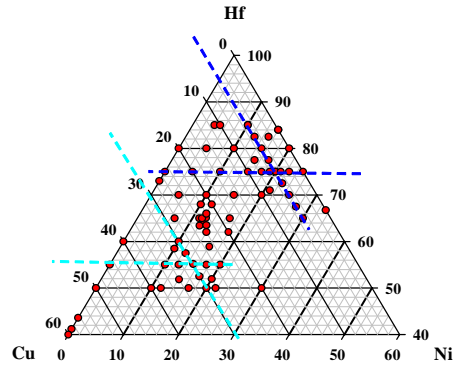






## Hf-Based BMGs

### The Search for the Invariant Points



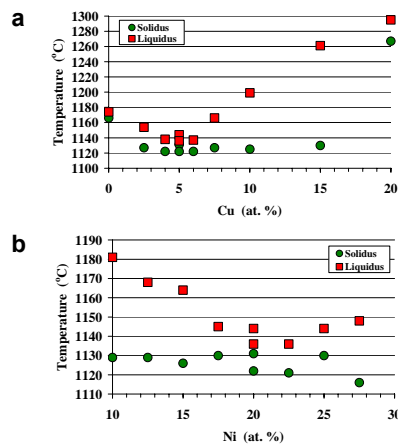
The locus of all experimentally fabricated Hf-Cu-Ni alloy points, depicted on the Hf-Cu-Ni ternary composition triangle.  
The sets of intersecting lines, define the invariant points found.

László Kecskés  
Army Science Conference #24 GO-03  
December 2, 2004

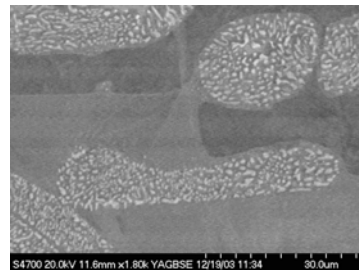


## Hf-Based BMGs

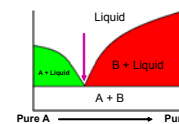
### The High-Hf Eutectic



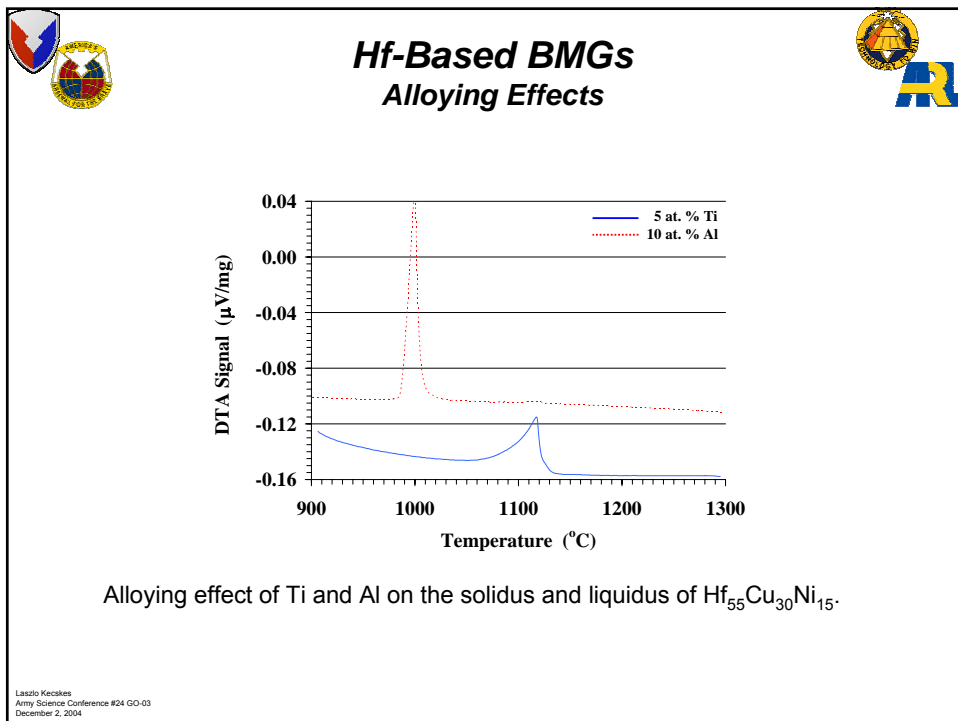
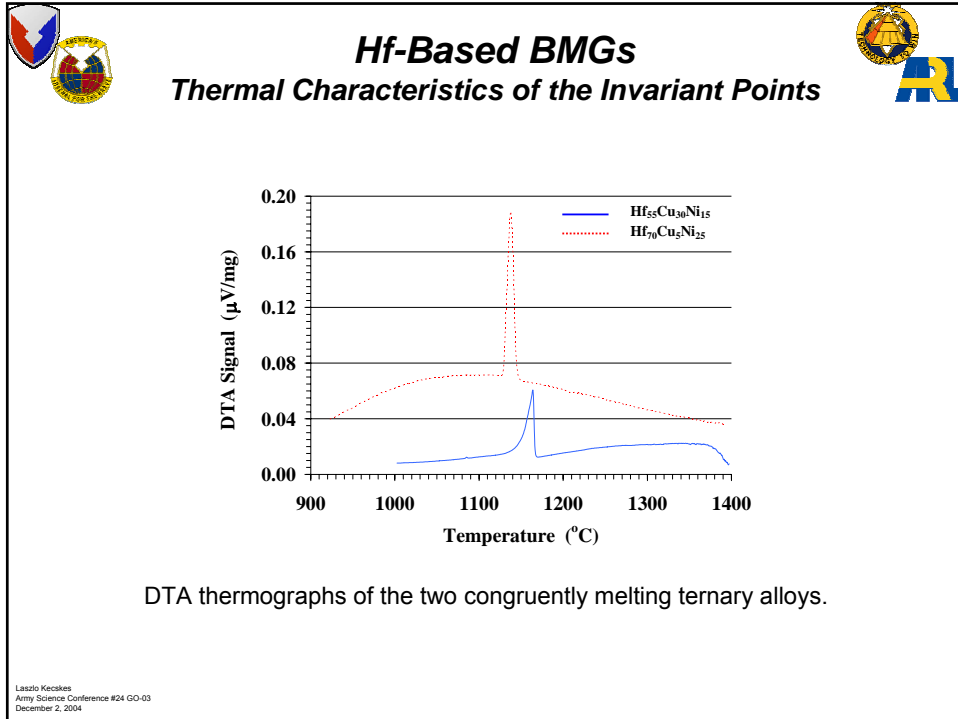
Plots of solidus and liquidus versus composition for  
(a)  $\text{Hf}_{75}\text{Cu}_x\text{Ni}_{25-x}$ , and  
(b)  $\text{Hf}_{95-x}\text{Cu}_5\text{Ni}_x$ .

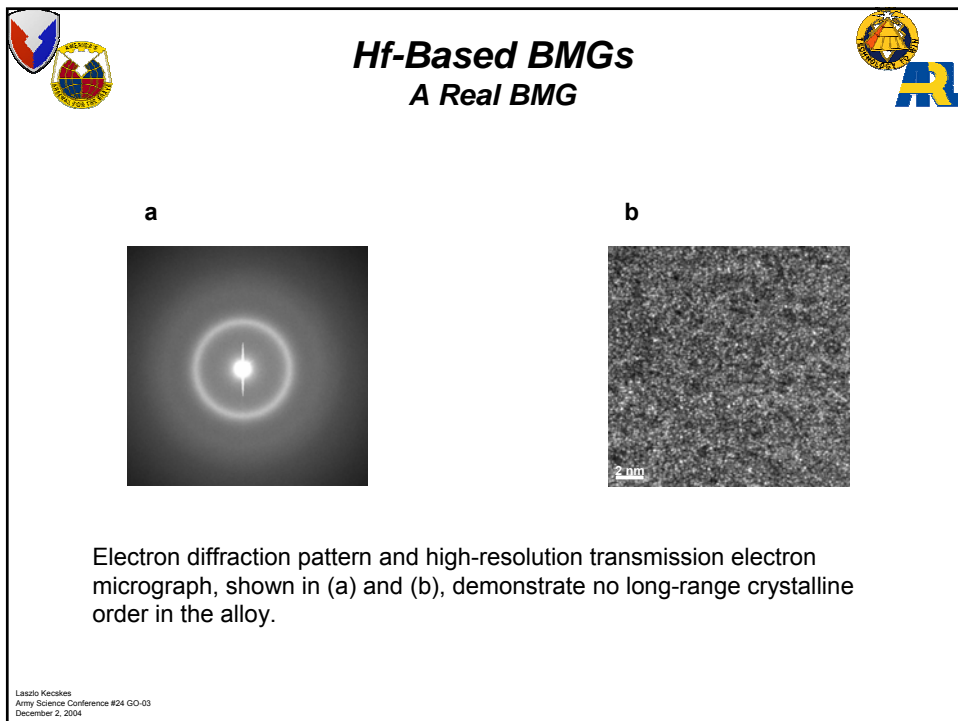
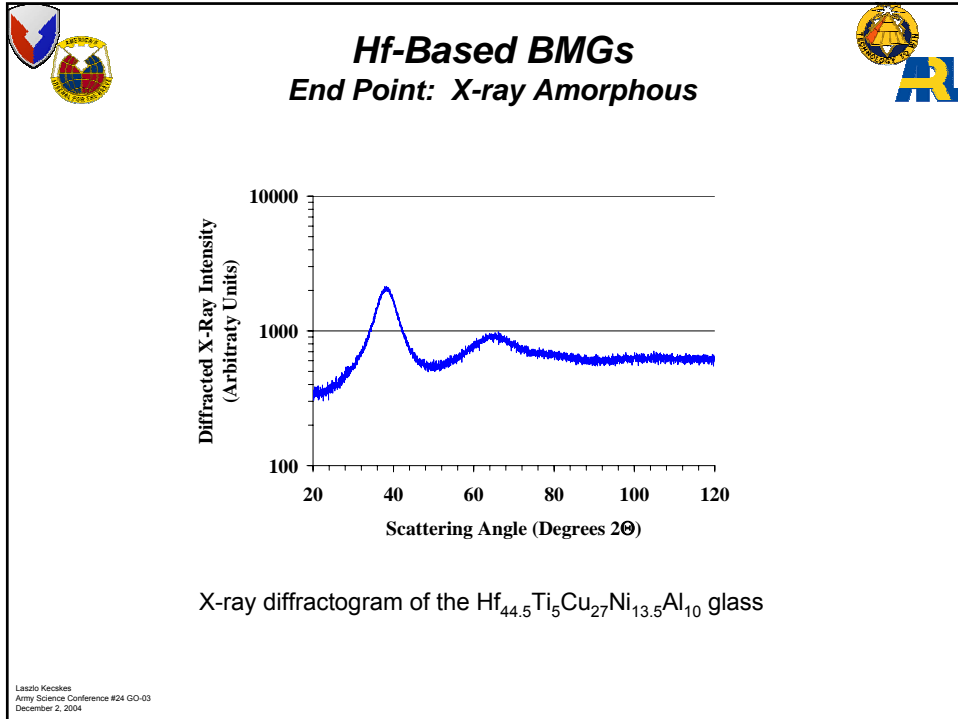


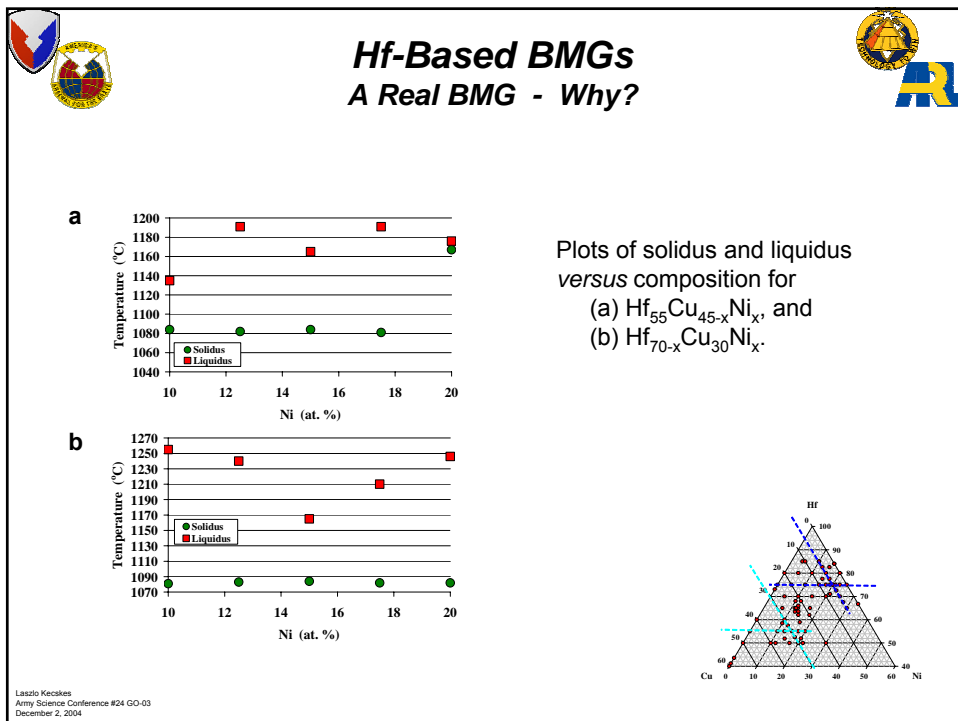
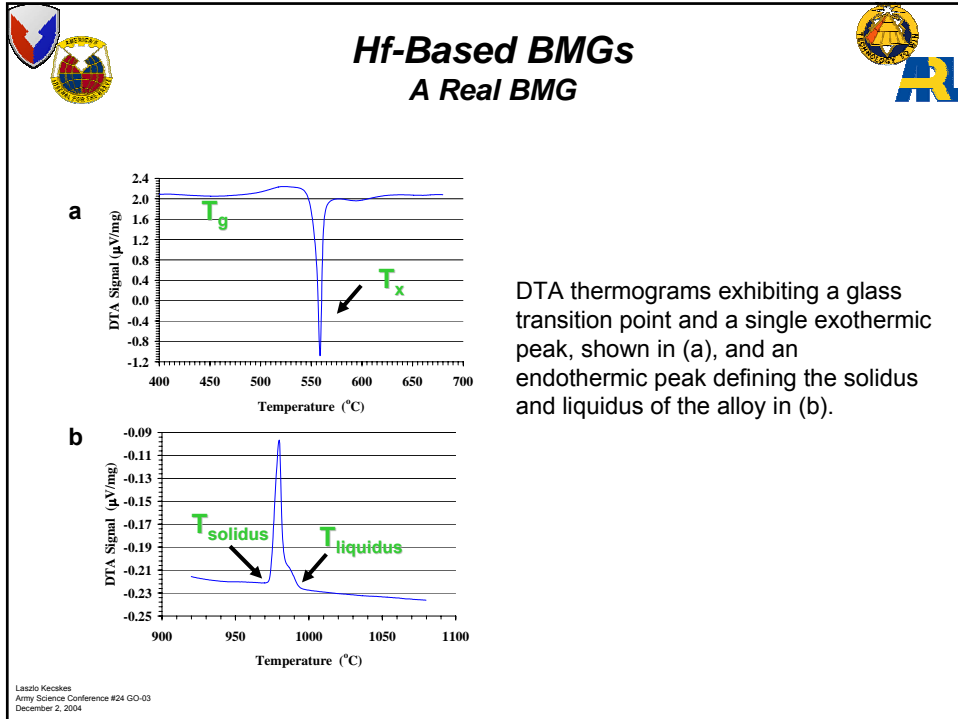
$\text{Hf}_{75}\text{Cu}_5\text{Ni}_{20}$

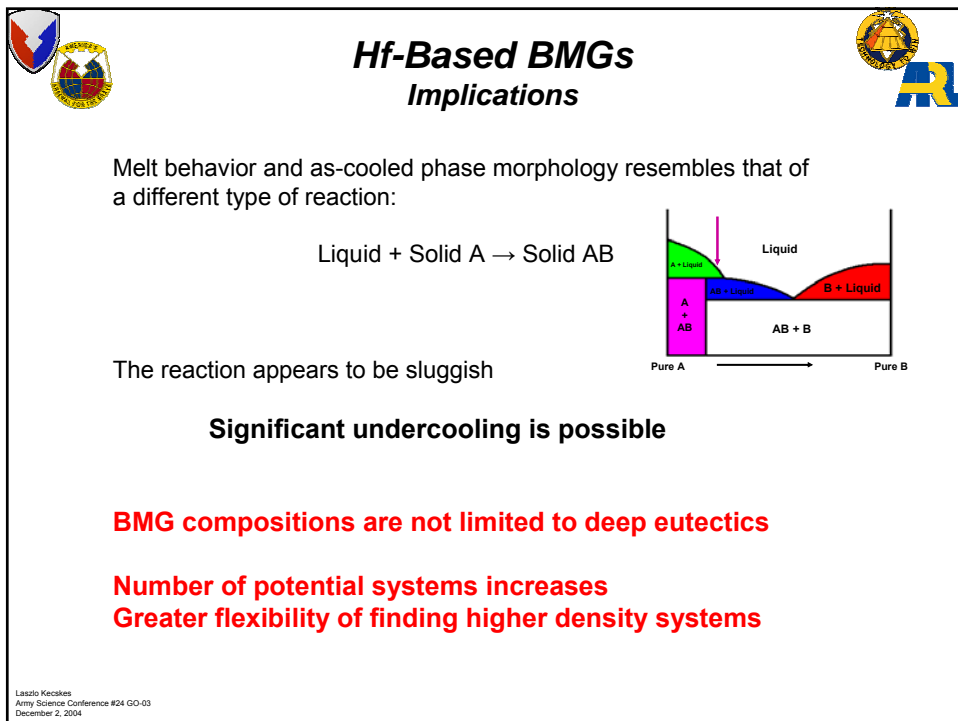
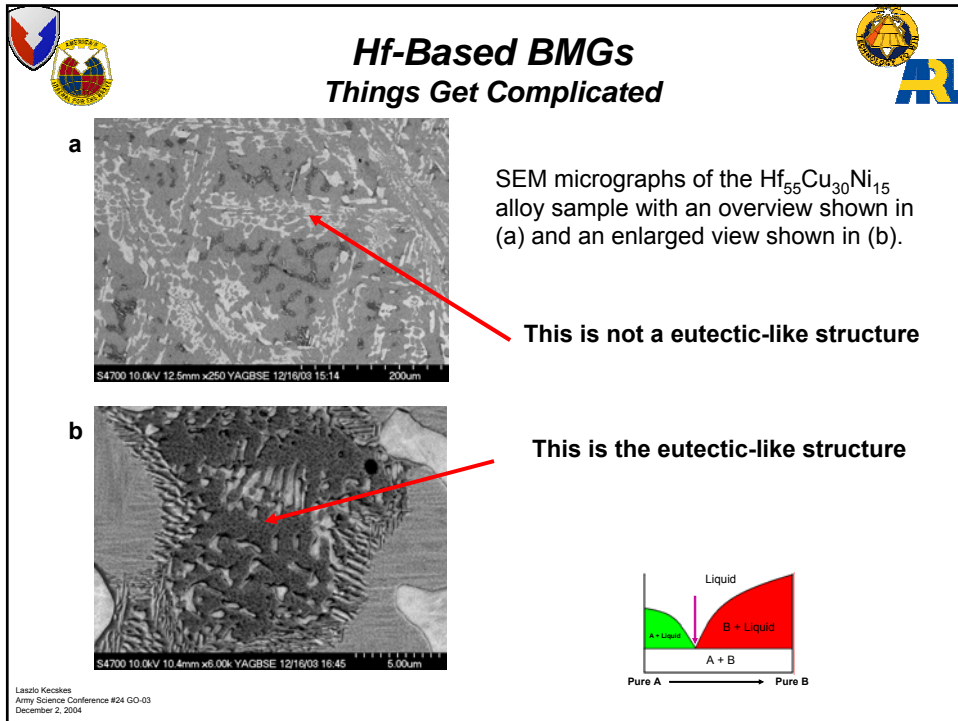


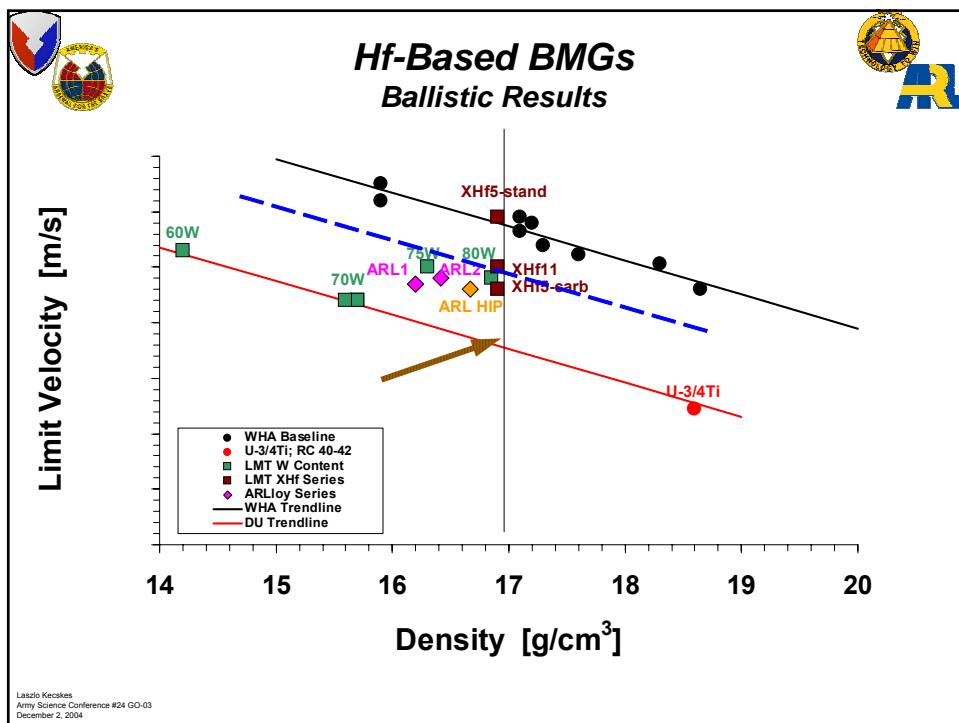
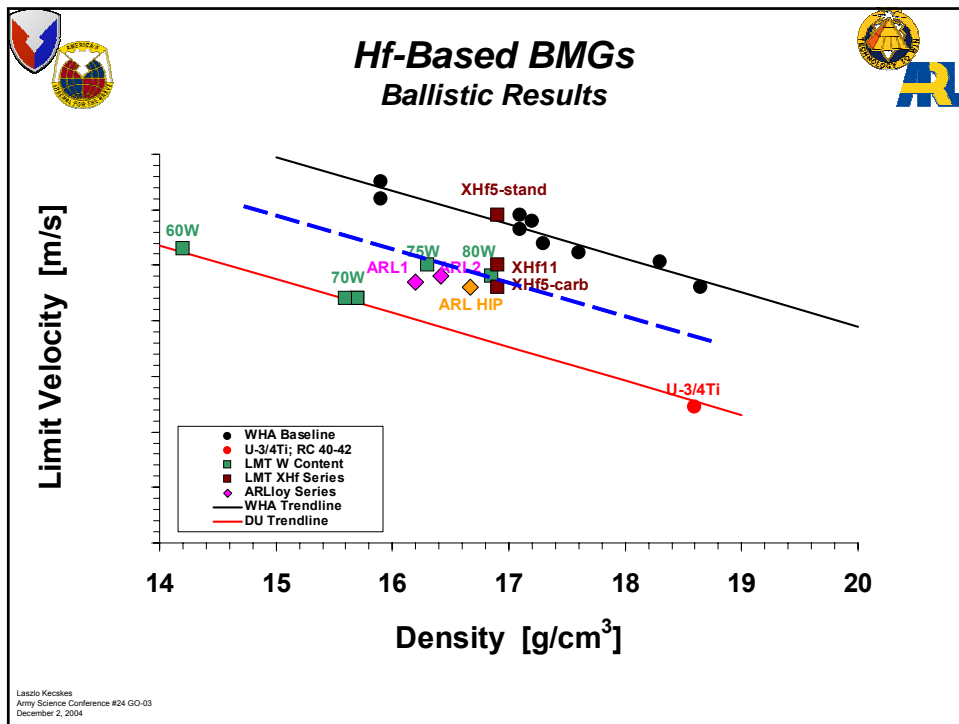
László Kecskés  
Army Science Conference #24 GO-03  
December 2, 2004













# Acknowledgements



Brad Klotz  
George Dewing  
John Brown